International Journal of Nanoelectronics and Materials

In Press, Accepted Manuscript – Note to user

High-Yield and Stepwise Synthesis of Graphene Oxide by Modified Hummers' Method

A.H. Surani[1], A. R. A Rashid[1,2*], N. Arshad[3] and A.A.N. Hakim[1]

[1]Faculty of Science and Technology, University Sains Islam Malaysia, 71800 Nilai, Negeri Sembilan.
[2]Frontier Materials Research Group (FMRG), Faculty of Science and Technology, Universiti Sains Islam Malaysia (USIM), Bandar Baru Nilai, Negeri Sembilan, Malaysia
[3]Faculty of Engineering and Built Environment, University Kebangsaan Malaysia, 43600 UKM Bangi, Selangor.

ABSTRACT

Graphene is a carbon-based material that has attracted tremendous attention due to its eccentric chemical and physical properties. Additionally, graphene can be converted into graphene oxide (GO) or reduced graphene oxide (rGO), depending on its application. In this paper, we report a simple step-by-step synthetisation of GO using Modified Hummers' method that enable the production of large scale by increasing the $KMnO_4$ ratio. The prepared GO was then characterised by FTIR spectra in order to confirm the functional groups of the prepared sample. UV-Vis characterisation was done and the results supported the FTIR results, confirming the existence of oxygen-functional groups. In addition, the prepared GO was characterised using XRD, FESEM, and RAMAN to investigate its interlayer distance, surface morphology, and structural information respectively.

Keywords: Graphene Oxide, Hummers' Method, FTIR, FESEM, RAMAN

1. INTRODUCTION

Carbon is widely dispersed throughout nature and it comes in different forms, called allotropes. From fullerenes to nanotubes, nanofibers to nanospheres, and the recent carbon allotrope that has been discovered, graphene [1]. Graphene can be obtained from nature in the form of graphite. It needs to be exfoliated from its precursor in order to get this magnificent material [2]. Graphene is described as a flat single layer of carbon atoms which are arranged in a two-dimensional (2D) honeycomb crystal lattice form. Each carbon atom in the honeycomb crystal lattice bonds with three other carbon atoms by sp^2-bonding [3]. Pristine graphene can transform into various forms like graphite (bulk of graphene), graphene oxide, and reduced graphene oxide depending on purposes and applications [4]. This transformation clearly visual in Figure 1.

Exfoliation of graphite by chemical oxidation leads to the formation of nanosheets of graphite oxide where oxygen- containing functional groups are introduced between layers of graphite [5]. Functional groups such as epoxy, hydroxyl, carboxyl, and carbonyl are attached on both sides of graphene sheets and their existence can be detected by Fourier-Transform Infrared Spectroscopy (FTIR) and recognised as major groups attached on it [6]. In addition, the interlayer spacing between lattices increases from 0.335 nm in graphite lattice to more than 0.625 nm in graphite oxide lattice [7].

*Corresponding Author: affarozana@usim.edu.my

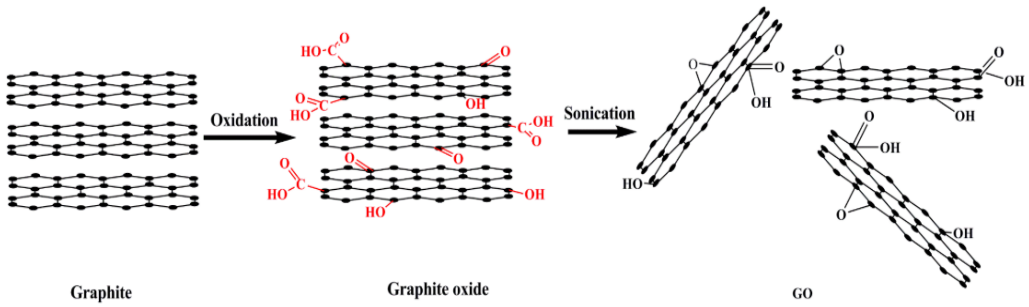

Figure 1. Oxidation of graphite to graphene oxide nanosheets [8].

As functional groups are intercalated between the graphite sheets, the Van der Walls forces between graphite become weaker. Graphite oxide can be easily exfoliated to form a multi-layer or single-layer nanostructure of graphene oxide by dispersing the graphite oxide in water assisted by sonication. This graphene oxide acquires multiple defects with different degrees of defecation depending on their oxidant amount and oxidising periods [9]. The presence of oxygen containing functional groups contributes to the hydrophilic properties of graphene oxide. Moreover, graphene oxide is easily dispersed in water and other organic solvents such as dimethylformamide (DMF) [10]. Upon its dispersion in different solvents, different long-term stability and thickness will be obtained. In fact, different solvents will produce different qualities of dispersion [11].

Graphene is an eccentric material with extraordinary characteristics, such as high-thermal conductivity (~5000 $Wm^{-1}K^{-1}$) and it tends to interact strongly with volatile organic compounds (VOC), especially with hydroxide (OH^-) or functional groups like carbonyl, carboxylic acid, and epoxy. This enables graphene to be able to distinguish different types of chemicals [12]. High surface-to-volume (2630 m^2g^{-1}) ratio is possible because graphene exhibits a structure of two dimensional sp^2 bond formed within a single layer of carbon atoms with each atom on the surface, thus making it an ideal candidate for a chemical vapor sensor. Other researchers reported that graphene surface is able to adsorb single gas molecules and this results in detectable changes in its electrical resistance. Therefore, graphene is outstanding as a chemical vapor sensor [13]. Magnificent optical transparency (~97.7%), excellent conductivity of electricity, and fast electron mobility are among the characteristics of graphene [14-15].

Synthesis of GO has gone through several evolutions. GO was first synthesised by Brodie in 1859 where graphite reacted with potassium chlorate ($KClO_3$) in fuming nitric acid (HNO_3) at a temperature of 60°C for 4 days. In 1898, Brodie's method was improved by Staudenmaier by replacing fuming HNO_3 with concentrated sulphuric acid (H_2SO_4) and multiplying the portion of $KClO_3$. This reaction took about 4 days to complete. 60 years later, Hummer and Offeman discovered a new improvement of Brodies's method by introducing potassium permanganate ($KMnO_4$) and sodium nitrate ($NaNO_3$) into their method. Through this harsh method, the long reaction time can be reduced from 4 days to only a few hours. The replacement of $KClO_3$ with $KMnO_4$ increased the safety of the reaction by eliminating the explosive chlorate (ClO_3) and usage of $NaNO_3$ eliminated toxic fog from HNO_3 [16]. This research attempts to synthesise large scale graphene oxide production using Modified Hummers' method by increasing the concentration ratio of $KMnO_4$ [9].

2. EXPERIMENTAL PROCEDURES

2.1 Materials

Graphite powder (99.0%, Acros Organics), sodium nitrate (84.99, R&M Chemicals), sulphuric acid (95.0%-98.0%, Alfa Aesar), potassium permanganate (≥99.0%, Sigma Aldrich), and hydrogen peroxide (27% w/w, Alfa Aesar).

2.2 Methodology

First, 5 g of graphite powder and 2.5 g of sodium nitrate ($NaNO_3$) were mixed in a 100 ml beaker. Next, 115 ml of sulphuric acid (H_2SO_4) was poured into the mixture. The solution was stirred by using magnetic stirrer for approximately 30 minutes. After that, the solution was kept for 30 minutes in the freezer before being transferred into an ice bath until the solution reached below 20° C. 15 g of potassium permanganate ($KMnO_4$) was slowly poured into the solution while the solution was constantly stirred. At this point, the solution turned from black to dark green. The solution then was transferred into a 35° C water bath and stirred for another 30 minutes. Besides producing bubbles, the solution at this moment will turn from dark green to purple brown and become thicker. Next, 230 ml of distilled water was added by using a dropper until the temperature of the solution reached 98° C. After the temperature increased, the solution was stirred again for 30 minutes. Another 400 ml of distilled water was added followed by 50 ml of hydrogen peroxide (H_2O_2). The solution was left for 24 hours to let the particles settle down in the beaker. The solution then washed by dilution of 100 ml hydrochloric acid (HCl) in 900 ml DI water. Following, 7 times by centrifugation before being dried in the oven overnight at 60° C. The GO sheets obtained were ground by mortar and pestle.

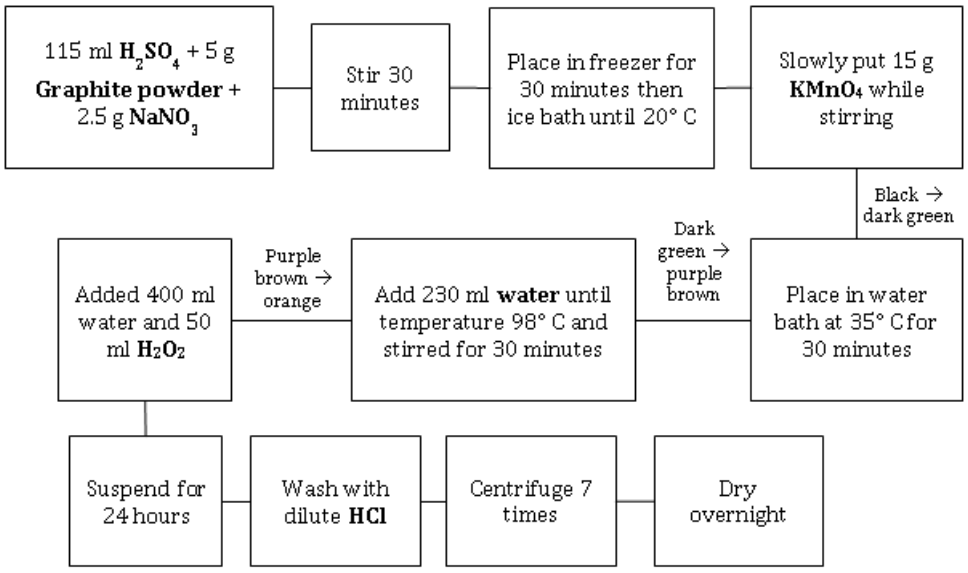

Figure 2. Flowchart representation of Modified Hummers' method.

2.3 Characterization

The synthesised graphene oxide nanosheets were characterised using x-ray diffractometer (XRD, D8 ADVANCE, Cu K-Alpha irradiation, λ= 0.15406 nm) to study the crystallographic structure of the graphene powder. Field emission scanning electron microscope (FESEM, GeminiSEM 500, Carl Zeiss) was used to observe the surface morphology and Raman microscope spectrometer (RAMAN, DXR Raman Microscope) with laser excitation wavelength of 532 nm was used to analyse structural information of the sample. Uv-Vis (Lambda 35, Perkin Elmer) was used to study the optical properties and Fourier transform infrared spectroscopy (FTIR, Nicolet 5700) was used to characterise the functional groups of graphene.

3. RESULTS AND DISCUSSION

3.1 FTIR Spectra

FTIR spectroscopy is one of the essential tools to characterize the functional groups of GO. The FTIR results of GO are shown in Fig. 1. The graph shows a broad peak of hydroxyl group (-OH) at 3429 cm^{-1} where it fell between the range of 3380-3390 cm^{-1}, indicating the presence of absorbed water molecules on the surface of GO. Therefore, it shows that this GO sample has strong hydrophilicity. The absorption peak at 1734 cm^{-1} represents the carbonyl group (C=O) where it fell between the range of 1720-1735 cm^{-1} that relates to carboxylic acid and its existence is at the edge of GO. Next, the absorption peak at 1621 cm^{-1} represents the graphitic domain where the range is between 1610-1625 cm^{-1} indicates the exfoliation happened where oxygen had been introduced during oxidation process thus contributes to the hydrophilic nature of GO sample [17]. Finally, the peak absorption at 1056 cm^{-1} corresponds to the presence of epoxy group (C-O-C), which lies between the range of 1050-1080 cm^{-1} [18]. According to Kim et al. (2010), hydrophilic nature of GO is cause by the existence of oxygen-containing polar groups like hydroxyl and carbonyl [19]. Therefore, the presence of these oxygen-containing groups such as hydroxyl, carbonyl and epoxy groups found in this study contribute to the hydrophilic nature of GO sample.

From the results of absorbance peaks obtained, it can be concluded that graphite had been successfully oxidized as it transformed into GO by the presence of oxygen functional groups. Through the oxidation process, oxygen molecules were attached at the edge of the graphite by weakening the Van Der Waal bond between graphite layers. It's clear that it is important to ensure the presence of oxygen molecules at the interlayer of graphite in order to transform graphite to GO [20].

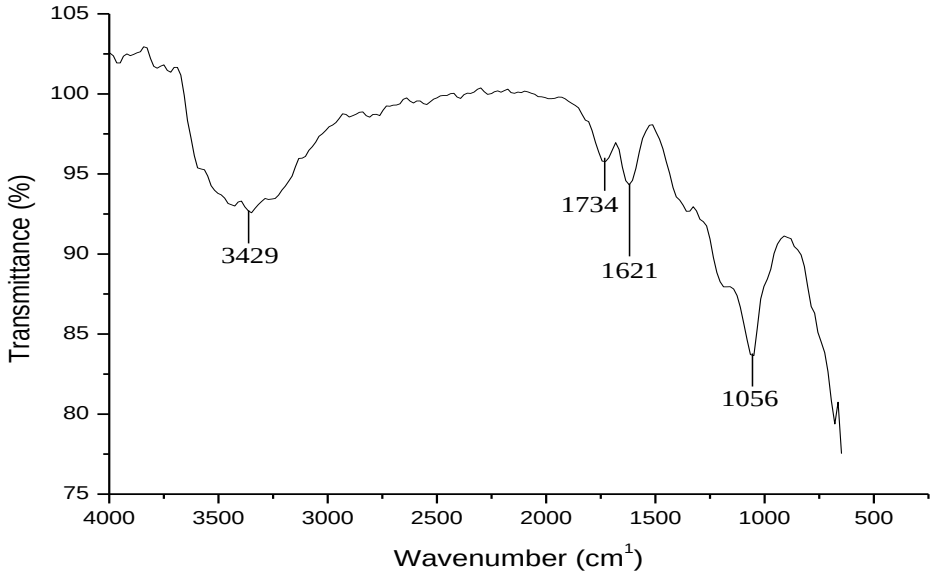

Figure 3. FTIR spectroscopy of GO nanosheets after dried in the oven overnight

3.2 UV-Vis Spectra

After 1 hour of sonication, the GO suspension was characterized by UV-Vis spectroscopy. The maximum absorption peak of GO can be observed at wavelength 230 nm which corresponds to the degree of remaining conjugation (π-π* transition of aromatic C-C bonds). Meanwhile, there was also a shoulder peak around 310 nm attributed to the n-π* transition of carbonyl group. Normally, thicker film exhibit higher absorbance value therefore the transparency is lower. In this prepared sample, the absorbance value is lower thus the transparency is higher. It is worth to mention that the prepared sample has higher transparency making them potentially advantageous in transparent conductive film application [21].

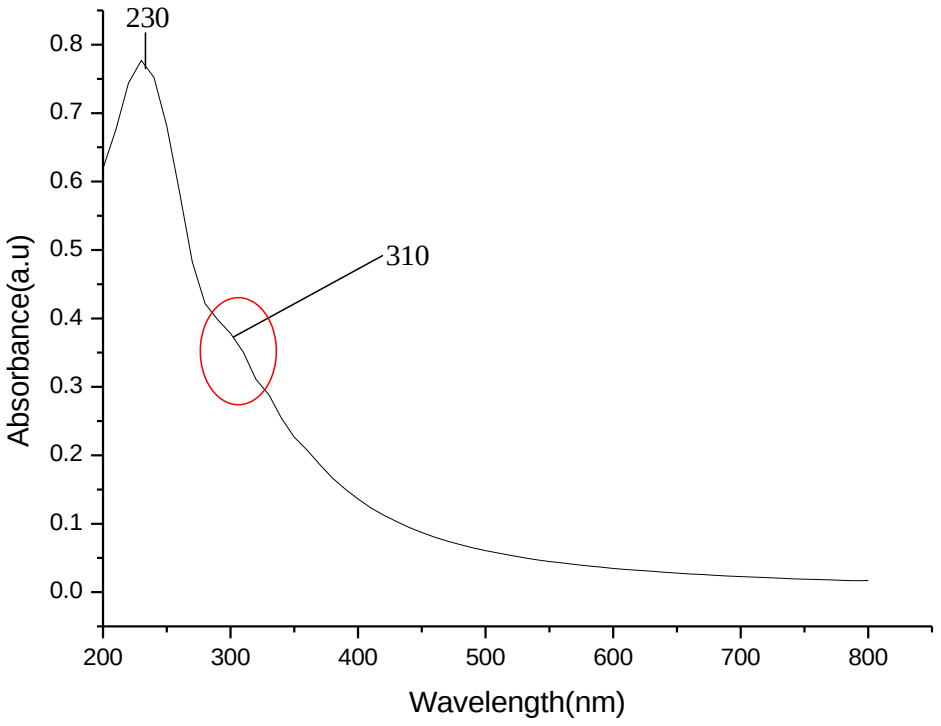

Figure 4. UV-Vis absorbance response of GO dispersion in distilled water after sonication of 1 hour through bath sonication.

3.3 XRD Patterns

From Figure 3, the graph shows XRD spectra for graphite and GO synthesised via modified Hummers' method respectively. According to the graph, the peak of the graphite is observed at $2\theta = 26.38º$. In consonance with Bragg's equation, $\lambda = 2d\sin(\theta)$ [22], where the wavelength of Cu Kα is 0.154 nm, the interlayer distance of graphite is 0.34 nm. It is contradictory with interlayer distance of GO where an intense and strong peak appears shifted to the left in the graph located at $2\theta = 11.3°$ with interlayer distance of 0.79 nm. The increase in interlayer distance revealed that the graphite precursor had been successfully oxidised to GO due to the intercalation of oxygen containing functional groups present between the precursor graphite crystalline structure [18]. This increase in interlayer distance make GO potentially desirable in membrane filtration field [23].

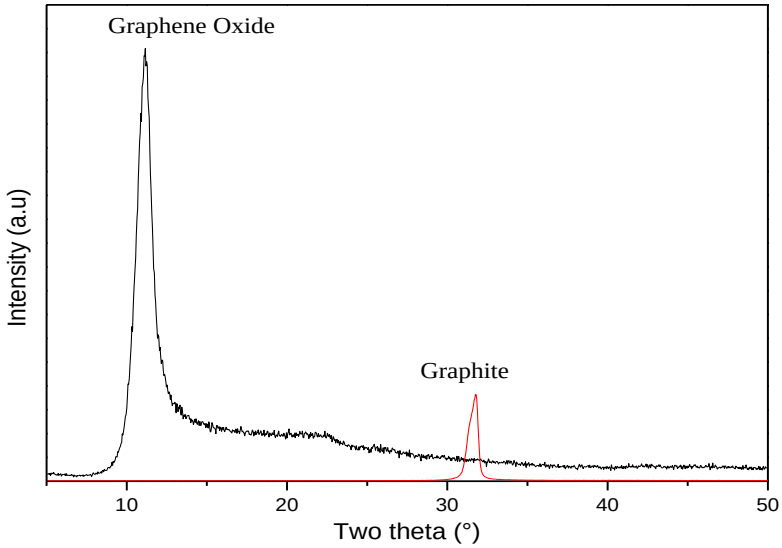

Figure 5. XRD spectra of GO and graphite powder as precursor

3.4 FESEM Images

FESEM was used in order to observe the surface morphology of GO. The FESEM photographs of GO at different magnifications are shown in Figure 3.4. From photograph A, surface of GO is creased and made of ridged structural layers which are overlapping with each other. Meanwhile, when the magnification of the photograph is increased, folded and continuous layers can be observed, as eloquently stated in another study [24] as GO possesses high surface area of thin film. This characteristic of GO is very significant in many application and one of them is in biosensor as high surface area increase the interaction between the functional groups with chemical molecule for example ethanol and benzene [14]. Besides, as GO possess good electrical conductivity in this high surface area, it is very popular in super-capacitor application as higher charge can be stored in it [25].

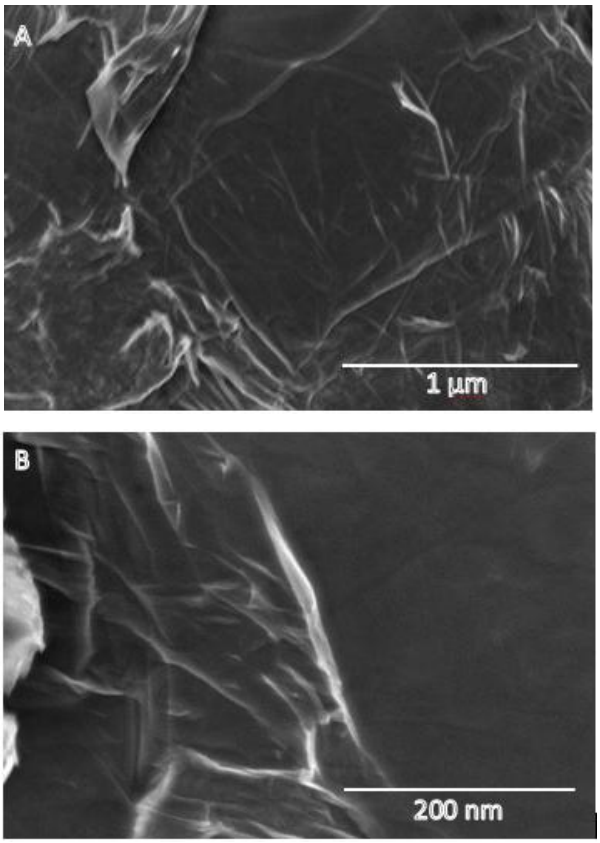

Figure 6. (A) FESEM image of GO sheets at magnification of 1µm and (B) FESEM image of GO sheets at magnification 200nm respectively.

3.5 RAMAN Spectra

Raman spectroscopy is a powerful non-destructive tool that is used extensively in order to gain structural information of carbon-based materials especially graphene [26]. Equally important, this graphitic carbon-based material can be easily discovered by the appearance of G and D bands followed by their overtones in the Raman spectra [27]. Figure 3.5 depicts the Raman spectra of GO with two prominent peaks corresponding to D band and G band appearing at 1348.06 cm^{-1} and 1587.07 cm^{-1} respectively. Shahriary and Athawale (2014) mentioned that both peaks are originating from the vibration of sp^2 carbon. The D band coincide to the arising of aromatic ring's breathing mode resulted in structural disorder of graphitic domain resulting from the introduction of hydroxyl and epoxide groups via the oxidation process [28]. Consequently, as mentioned by [29], D band is also the result of breathing mode of k-points phonons with A_{1g} symmetry. On the other hand, G band peak is associated with the first order scattering of E_{2g} phonons in the sp2 bonded carbon [30]. As demonstrated, the intensity ratio of the I_D/I_G band is 0.8 which corresponds to the degree of disorder where there are generous amounts of defects introduced in the GO which happened during the oxidation process [31].

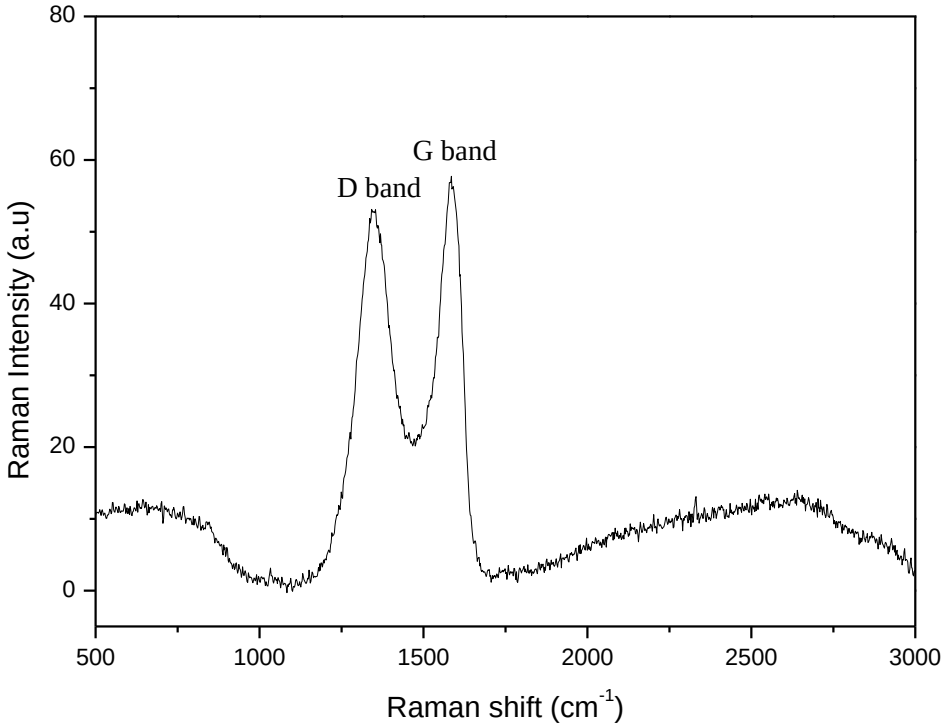

Figure 7. Raman spectra of GO powder

4. CONCLUSION

In summary, GO nanosheets were prepared by Hummers' method in this study by exfoliating graphite powder using a strong oxidising agent, that is sulphuric acid. The process was simple yet produced high yield. In this study, hydroxyl, carbonyl, and epoxy groups were detected by FTIR spectroscopy at wavelengths between 800 cm^{-1} to 4000 cm^{-1}. In addition, the XRD pattern of the prepared GO shows an increase in interlayer distance, indicating the introduction of oxygen containing functional groups between the GO nanosheets. Absorbance peak of GO at 230 nm wavelength detected by UV-Vis supports the detection of oxygen functional groups by FTIR spectroscopy. Through FESEM, the surface morphology of the prepared GO can be observed as crumpled and continuous layers proved the high surface area possessed by the sample. Lastly, the prepared sample exhibits 2 dominant D-band and G-band at 1348.06 cm^{-1} and 1587 cm^{-1} respectively. Therefore, the prepared GO has been successfully synthesised from graphite precursor through Hummers' method.

ACKNOWLEDGEMENTS

The authors would like to thank Universiti Sains Islam Malaysia (USIM) and staff for guidance and assistance. This project was sponsored by the Kementerian Pendidikan Malaysia (KPM) through grant scheme (USIM/RAGS/FST/36/50215) and (GUP-2017-059) from UKM.

REFERENCES

[1] Del Prado Lavín López, M., Luis Valverde Palomino, J., Sánchez-Silva, L., Romero Izquierdo,A., Optimization of the Synthesis Procedures of Graphene and Graphite Oxide, Recent Advances in Graphene Research, Intech, 2016, 114-133.

[2] Segal, M., Nat. Nanotechnol. **4** (2009) 612.
[3] Geim, A. K. N., Novoselov, K. S., Nat. Mater. **6** (2007) 183-191.
[4] Zahed. M., Sadat Parsamehr, P., Tofighy, M. A., Mohammadi, T., Chem. Eng. Res. Des. (2018).
[5] Oliveira, A. E. F., Braga, G. B., Tarley, C. R. T., Pereira, A. C., J. Mater. Sci. **53** (2018) 12005-12015.
[6] Singh, R. K., Kumar, R. Singh D. P., RSC Adv. **6** (2016) 64993-65011
[7] Hontoria-Lucas, C., López-Peinado, A. J., López-González, J. d. D., Rojas-Cervantes, M. L., Martín-Aranda, R. M., Carbon N. Y. **33** (1995) 1585-1592.
[8] Li, J., Zeng. X., Ren, T., Van Der Heide, E., Lubricants. **2** (2014).
[9] Arthi G, P. B., BD, L., J. Nanomed. Nanotechnol. **6** (2015) 2-5.
[10] Sharma, N., Sharma, V., Jain, Y., Kumari, M., Gupta, R., Sharma, S. K., Sachdev, K., Macromol. Symp. **376** (2017) 1700006.
[11] Zaaba, N. I., Foo, K. L., Hashim, U., Tan, S. J., Liu, W. W., Voon, C. H., Procedia Eng. **184** (2017) 469-477
[12] Rosli, M. A. A., Arasu, P. T., Lim, H. N., Noor, A. S. M., 2016 IEEE 6th Int. Conf. Photonics, ICP 2016 (2016) 16-18.
[13] Zhang, H., Kulkarni, A., Kim, H., Woo, D., Kim, Y. J., Hong, B. H., Choi, J. B., Kim, T., J. Nanosci. Nanotechnol. **11** (2011) 5939-5943.
[14] Gao, S. S., Qiu, H. W., Zhang, C., Jiang, S. Z., Li, Z., Liu, X. Y., Yue, W. W., Yang, C., Huo, Y. Y., Feng, D. J., Li, H. S., RSC Adv. **6** (2016) 15808-15815.
[15] Batumalay, M., Harith, Z., Rafaie, H. A., Ahmad, F., Khasanah, M., Harun, S. W., Nor, R. M., Ahmad, H., Sensors Actuators, A Phys. **210** (2014) 190-196.
[16] Chen, J., Yao, B., Li, C., Shi, G., Carbon N. Y. **64** (2013) 225-229.
[17] Hu, X., Yu, Y., Zhou, J., Song, L., Nano. **9** (2014) 1450037
[18] Bhawal, P., Ganguly, S., Chaki, T. K., Das, N. C., RSC Adv. **6** (2016) 20781-20790.
[19] Kim, J., Cote, L. J., Kim, F., Yuan, W., Shull, K. R., Huang, J., Chem. Soc. **132** (2010) 8180-8186
[20] Chong, S. W., Lai, C. W., Abd Hamid, S. B., Low, F. W., Liu, W. W., Adv. Mater. **1109** (2015) 390-394
[21] Lai, Q., Zhu, S., Luo, X., Zou, M., Huang, S., AIP Adv. **2** (2012) 3-8.
[22] Zheng, Q., Li, Z., Yang, J., Kim, J. Elsevier Ltd. **64** (2014) 200-247
[23] Rattana, T., Chaiyakun, S., Witit-anun, N., Nuntawong, N., Chindaudom, P., Oaew, S., Kedkeaw, C., Limsuwan, P., Procedia Eng. **32** (2012) 759-764.
[24] Li, W., Wu, W., Li, Z. ACS Nano. **12** (2018) 9309-9317
[25] Girei, S. H., Shabaneh, A. A., Ngee-Lim, H., Hamidon, M. N., Mahdi, M. A., Yaacob, M. H., Opt. Rev. **22** (2015) 385-392.
[26] Tuz Johra, F., Lee, J., Jung, W. G., Journal of Industrial and Engineering Chemistry. **20** (20140.
[27] Kumar Gupta, D., Singh Rajaura, R., Sharma, K., Suresh Gyan Vihar Univ. Int. J. Environ. Sci. Technol. 1 (2015) 16-24.
[28] Shahriary, L., Athawale, A. A., Int. J. Renew. Energy Environ. Eng. 2 (2014), 58-63.
Low, F. W., Lai, C. W., Abd Hamid, S. B., Chong, S. W., Liu, W. W., Adv. Mater. Res. 1109 (2015) 385-389.
[29] Kellici, S., Acord, J., Ball, J., Reehal, H. S., Morgan, D., Saha, B., RSC Adv. 4 (2014) 58-63.
[30] Aziz, A., Lim, H. N., Girei, S. H., Yaacob, M. H., Mahdi, M. A., Huang, N. M., Pandikumar, A., Sensors Actuators, B Chem, **206** (2015) 119-125.
[31] Xu, J., Liu, J., Wu, S., Yang, Q. H., Wang, P., Opt. Express. **20** (2012) 15474-15480.
[32] Yu, H., Zhang, B., Bulin, C., Li, R., Xing, R., Sci. Rep. **6** (2016) 36143.